Accepted Manuscript

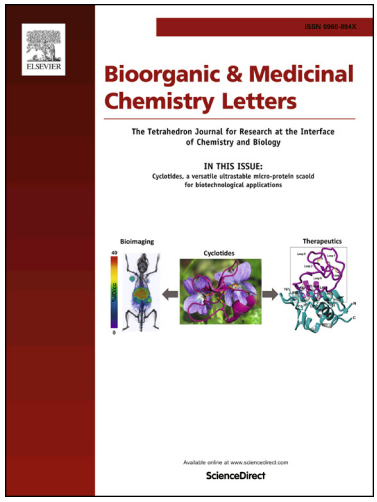

Identification of Bicyclic Hexafluoroisopropyl Alcohol Sulfonamides as Retinoic Acid Receptor-Related Orphan Receptor Gamma (RORγ/RORc) Inverse Agonists. Employing Structure-Based Drug Design to Improve Pregnane X Receptor (PXR) Selectivity

Hua Gong, David S. Weinstein, Zhonghui Lu, James J.-W. Duan, Sylwia Stachura, Lauren Haque, Ananta Karmakar, Hemalatha Hemagiri, Dhanya Kumar Raut, Arun Kumar Gupta, Javed Khan, Dan Camac, John S. Sack, Andrew Pudzianowski, Dauh-Rurng Wu, Melissa Yarde, Ding-Ren Shen, Virna Borowski, Jenny H. Xie, Huadong Sun, Celia D'Arienzo, Marta Dabros, Michael A. Galella, Faye Wang, Carolyn A. Weigelt, Qihong Zhao, William Foster, John E. Somerville, Luisa M. Salter-Cid, Joel C. Barrish, Percy H. Carter, T.G. Murali Dhar

PII: S0960-894X(17)31166-6
DOI: https://doi.org/10.1016/j.bmcl.2017.12.006
Reference: BMCL 25462

To appear in: *Bioorganic & Medicinal Chemistry Letters*

Received Date: 4 October 2017
Revised Date: 18 November 2017
Accepted Date: 4 December 2017

Please cite this article as: Gong, H., Weinstein, D.S., Lu, Z., J.-W. Duan, J., Stachura, S., Haque, L., Karmakar, A., Hemagiri, H., Kumar Raut, D., Kumar Gupta, A., Khan, J., Camac, D., Sack, J.S., Pudzianowski, A., Wu, D-R., Yarde, M., Shen, D-R., Borowski, V., Xie, J.H., Sun, H., D'Arienzo, C., Dabros, M., Galella, M.A., Wang, F., Weigelt, C.A., Zhao, Q., Foster, W., Somerville, J.E., Salter-Cid, L.M., Barrish, J.C., Carter, P.H., Murali Dhar, T.G., Identification of Bicyclic Hexafluoroisopropyl Alcohol Sulfonamides as Retinoic Acid Receptor-Related Orphan Receptor Gamma (RORγ/RORc) Inverse Agonists. Employing Structure-Based Drug Design to Improve Pregnane X Receptor (PXR) Selectivity, *Bioorganic & Medicinal Chemistry Letters* (2017), doi: https://doi.org/10.1016/j.bmcl.2017.12.006

Bioorganic & Medicinal Chemistry Letters
journal homepage: www.elsevier.com

Identification of Bicyclic Hexafluoroisopropyl Alcohol Sulfonamides as Retinoic Acid Receptor-Related Orphan Receptor Gamma (RORγ/RORc) Inverse Agonists. Employing Structure-Based Drug Design to Improve Pregnane X Receptor (PXR) Selectivity

Hua Gong,[a] David S. Weinstein,[a] Zhonghui Lu,[a] James J.-W. Duan,[a] Sylwia Stachura,[a] Lauren Haque,[a] Ananta Karmakar,[b] Hemalatha Hemagiri,[b] Dhanya Kumar Raut,[b] Arun Kumar Gupta,[b] Javed Khan,[a] Dan Camac,[a] John S. Sack,[a] Andrew Pudzianowski,[a] Dauh-Rurng Wu,[a] Melissa Yarde,[a] Ding-Ren Shen,[a] Virna Borowski,[a] Jenny H. Xie,[a] Huadong Sun,[a] Celia D'Arienzo,[a] Marta Dabros,[a] Michael A. Galella,[a] Faye Wang,[a] Carolyn A. Weigelt,[a] Qihong Zhao,[a] William Foster,[a] John E. Somerville,[a] Luisa M. Salter-Cid,[a] Joel C. Barrish,[a] Percy H. Carter[a] and T. G. Murali Dhar*[a]

[a] *Bristol-Myers Squibb, Research and Development, Princeton, New Jersey 08543-4000, United States.* [b] *Bristol-Myers Squibb-Biocon Research Center, Bangalore, India.*
** Corresponding author: murali.dhar@bms.com*

Article history:
Received
Revised
Accepted
Available online

Keywords: ROR, retinoic acid-related orphan receptor; PXR, pregnane X receptor; LXR, liver X receptor; IBD, inflammatory bowel disease; RA, rheumatoid arthritis, MS, multiple sclerosis.

We disclose the optimization of a high throughput screening hit to yield benzothiazine and tetrahydroquinoline sulfonamides as potent RORγt inverse agonists. However, a majority of these compounds showed potent activity against pregnane X receptor (PXR) and modest activity against liver X receptor α (LXRα). Structure-based drug design (SBDD) led to the identification of benzothiazine and tetrahydroquinoline sulfonamide analogs which completely dialed out LXRα activity and were less potent at PXR. Pharmacodynamic (PD) data for compound **35** in an IL-23 induced IL-17 mouse model is discussed along with the implications of a high Y_{max} in the PXR assay for long term preclinical pharmacokinetic (PK) studies.

The retinoic acid-related orphan receptors belong to the NR1F subfamily of nuclear hormone receptors. All three members – RORα (NR1F1), RORβ (NR1F2), and RORγ (NR1F3) play important roles in organ development, immunity, metabolic regulation, neural function, and circadian rhythms.[1] RORγt and RORγ (RORc in human) are two splice variants that are identical apart from an N-terminal extension of 24 amino acids present only in RORγ. RORγ is highly expressed in the thymus in addition to kidney, liver, pancreas, muscle, and adipose, whereas the expression of RORγt is restricted to lymphoid cells. RORγ regulates the expression of genes that control metabolism in skeletal muscle and fat and that regulate circadian rhythms in non-immune cells. The normal differentiation and/or function of specialized lymphocytes including IL-17 producing T helper (Th17) cells, innate lymphoid cells (ILC), γδ cells and the development of lymph nodes is dependent on RORγt. Importantly, RORγt regulates the expression of pro-inflammatory cytokines such as IL-17A,[2] IL-17F, IL-22 and GM-CSF that are implicated in several inflammatory and autoimmune diseases such as psoriasis, inflammatory bowel disease (IBD), rheumatoid arthritis (RA), and multiple sclerosis (MS).[3]

Findings from numerous studies with RORγt-deficient mice suggest that RORγt is a critical component in the pathogenesis of a range of immune and inflammatory diseases, including psoriasis, IBD, MS, graft versus host disease (GvHD), nephritis, asthma and cancer.[4] Several small molecule inverse agonists of RORγt, have shown robust efficacy in preclinical models of psoriasis,[5] IBD,[6] RA[5c,6a,7,8a] and MS.[8] In these preclinical studies, reduced disease severity is accompanied by a decrease in Th17-related cytokines. Taken together, both genetic and pharmacologic evidence support the potential for broad clinical utility of RORγt inverse agonists for the treatment of a variety of immune-related disorders.[3,9,10] It is therefore not surprising that a few compounds are already in clinical development, the most advanced being (*S*)-*N*-((5-(ethylsulfonyl)pyridin-2-yl)methyl)-7-isopropyl-6-(((1*r*,4*S*)-4-(trifluoromethyl)cyclohexyl)methyl)-6,7-dihydro-5*H*-pyrrolo[3,4-*b*]pyridine-3-carboxamide (VTP-43742).[11,12]

Herein we report the structure-activity relationships (SAR) and SAR-based optimization of a HTS hit to yield potent and selective inverse agonists of RORγt. We used reporter assays to

characterize the *in vitro* biological activities of RORγt ligands including both potency and selectivity. A Jurkat cell based Gal4 reporter assay was used to measure RORγt-dependent transcriptional luciferase activity driven by the native IL-17 promoter (see supplementary material section). Functional LXR α/β isoform activity was assessed using LXRα and LXRβ transactivation assays in CV-1 cells.[13] Functional PXR activity was assessed using a transactivation assay in HepG2 cells.[14] *N*-(4-(1,1,1,3,3,3-hexafluoro-2-hydroxypropan-2-yl)phenyl)-*N*-(2,2,2-trifluoroethyl)benzenesulfonamide (T0901317)[15] was employed as the positive control for the RORγt inverse agonist assay.

A HTS campaign of the Bristol-Myers Squibb (BMS) compound deck identified compound **1** as a potential lead with an EC_{50} of 165 nM in the Gal4 reporter assay for RORγt (Table 1). In addition, compound **1** was significantly less potent against RORα and RORβ in cellular assays (EC_{50} > 20 μM) and had no activity in the agonist mode for RORα, RORβ and RORγt at the concentrations tested (EC_{50} > 40 μM). The functional selectivity of compound **1** for RORα/β, in both the agonist and the inverse agonist mode, may be due to the differential recruitment of co-activators/co-repressors for RORγt vs. that for RORα/β. However, compound **1** showed significant activity against PXR, LXRα and LXRβ in the agonist mode (Table 1). We envisioned that the PXR and LXRα/β activities can potentially be minimized while optimizing the potency of compound **1** for RORγt. Table 1 outlines the SAR of the core modifications and its impact on RORγt activity and selectivity for PXR and LXRα/β. It is clear from the SAR shown in Table 1 that changes to the core did not significantly alter the potency of the compounds for RORγt nor improve the selectivity vs. PXR and LXRα/β. The SAR data also indicates that the compounds were more potent at PXR than at RORγt or LXRα/β.

Table 1. Core modification SAR

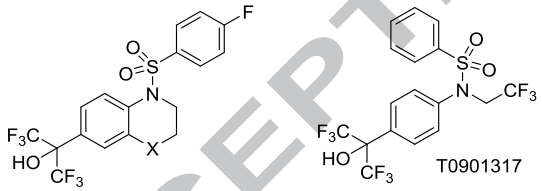

T0901317

	X	RORγt EC_{50} nM[a,b]	PXR EC_{50} nM (% max.)[c]	LXRα EC_{50} nM (% max.)[d]	LXRβ EC_{50} nM (% max.)[d]
T0901317		333 ± 48	8 (84)	359 ± 15 (~90)[a]	198 ± 19 (~100)[a]
1	S	165 ± 40	20 (100)	190 ± 34 (80)[a]	185 ± 15 (100)[a]
2	O	203 ± 9	ND	265 (78)[c]	340 (86)[c]
3	NH	600[c]	ND	310 (64)[c]	445 (64)[c]
4	NMe	170 ± 34	18 (100)	385 (47)[c]	455 (75)[c]
5	CH_2	280 ± 135	25 (100)	163 ± 74 (70)[a]	223 ± 75 (99)[a]
6	CHMe[e]	195 ± 63	16 (100)	70 (60)[c]	130 (70)[c]
7	$C(Me)_2$	815[c]	36 (100)	290 (39)[c]	550 (80)[c]

[a]Values are means of two or more experiments performed in triplicate. [b]RORγt reporter assay was performed using a Jurkat cell line. [c]value from a single experiment performed in duplicate. [d]LXR assays (agonist mode) were performed using a CV-1 cell line. eracemic. ND = not determined

Before embarking on further SAR work around the cores shown in Table 1, we decided to briefly explore the SAR around the 4-fluorophenylsulfone moiety of **1** to determine the optimal substitution pattern required for potency in this region of the molecule (Table 2).

Substituting the sulfone moiety of compound **1** with a carbonyl group leads to loss of activity at RORγt (compound **8**) suggesting that the tetrahedral nature of the sulfone may be responsible for projecting the 4-fluorophenyl group for optimal interactions with the ligand binding domain (LBD) of RORγt (*vide infra*). It is interesting to note that the 2-fluoro and 3-fluoro substitution patterns lead to significant loss in potency compared to the 4-fluoro analog (compare **11** and **12** with **1**). The loss in potency with the 2-fluoro analog **11** may be attributed to the distortion in orientation of the phenyl group due to repulsive interactions of the fluoro moiety with the sulfone oxygens (*vide infra*). However, the loss in potency with the 3-fluoro analog **12** is not obvious. The 4-chlorophenyl and chloropyridyl analogs (compounds **13** and **16** respectively), were equipotent to **1**. In contrast to the parent phenyl analog **10** which had similar potency to the 4-fluoro analog **1**, the pyridyl analog **15** was inactive in the RORγt reporter assay, probably due to the hydrophobic nature of the pocket in this region of the LBD (*vide infra*). Although, the desfluoro, 4-chloro and the chloropyridyl analogs (**10**, **13** and **16** respectively) were similar in potency to **1**, they did not offer any advantage in terms of reduced potency at LXRα/β and PXR (data not shown).

Table 2. SAR of benzothiazine sulfonamides

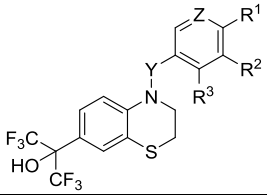

	Y	Z	R^1	R^2	R^3	RORγt EC_{50} nM[a,b]
1	SO_2	CH	F	H	H	165 ± 40
8	C=O	CH	F	H	H	>10000
9	CH_2	CH	F	H	H	>10000
10	SO_2	CH	H	H	H	230 ± 80
11	SO_2	CH	H	H	F	1260[b]
12	SO_2	CH	H	F	H	2040 ± 1570
13	SO_2	CH	Cl	H	H	165 ± 80
14	SO_2	CH	OMe	H	H	530 ± 175
15	SO_2	N	H	H	H	>10000
16	SO_2	N	Cl	H	H	170[b]

[a]Values are means of two or more experiments performed in triplicate. [b]Value from a single experiment performed in duplicate.

Since X-ray co-crystal structures with the LBD's of RORγt and/or PXR were not available at this point in the program, we decided to conduct SAR empirically at the 2-position of compound **1** in order to improve the potency of compounds for RORγt while reducing the LXRα/β and PXR activity. Although various groups were considered, we decided to pursue the acetic

acid analog **18**, since it was easily accessible and the acid moiety enabled us to quickly evaluate SAR. A number of analogs were synthesized and evaluated for potency vs. RORγt. Table 3 summarizes data for a representative set of compounds.

Table 3. SAR of 2-substituted benzothiazine sulfonamides

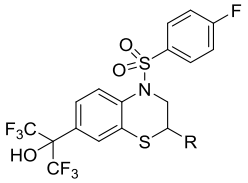

	X	RORγt EC_{50} nM[a,b]	PXR EC_{50} nM (% max.)[c]	LXRα EC_{50} nM (% max.)[d]	LXRβ EC_{50} nM (% max.)[d]
1	H	165 ± 40	20 (100)	190 ± 34 (80)[a]	185 ± 15 (100)[a]
17	$-CH_2CO_2Me$	93 ± 15	55 (100)	250 ± 90 (75)[a]	370 ± 28 (86)
18	$-CH_2CO_2H$	2780[c]	ND	>7500[c]	>7500[c]
19	$-CH_2CONH_2$	240[c]	190 (100)	970 (50)[c]	2820 (36)[c]
20	$-CH_2CONHMe$	225[c]	ND	2403 ± 1340 (48)[a]	2470 ± 40 (30)[a]
21	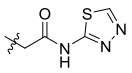	84[c]	254 (100)	342 ± 54 (23)[a]	2900 (15)[c]
22	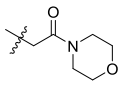	58[c]	380 (100)	980 ± 0.27 (40)	2450 ± 45 (20)[c]
23	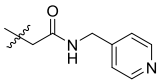	28[c]	250 (100)	2070 ± 5 (27)	3120±120 (100)
24	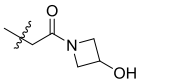	114[c]	ND	1300 (30)[c]	>7500[c]
25	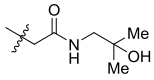	31 ± 12	175 (90)	2770 ± 600 (39)	>7500
25a[†]	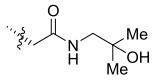	12 ± 7	144 (100)	2820 ± 1275 (40)	>7500
25b	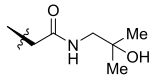	1640[c]	228 (82)	3280 (34)[c]	>7500
26	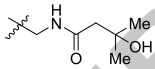	80[c]	520 (100)	374 (74)[c]	1040 (95)[c]

**All compounds shown in the table are racemic except for 25a and 25b. [a]Values are means of two or more experiments performed in triplicate. [b]RORγt reporter assay was performed using a Jurkat cell line. [c]Value from a single experiment performed in duplicate. [d]LXR assays (agonist mode) were performed using a CV-1 cell line. [†]Absolute stereochemistry established by single crystal X-ray (CCDC # 1586092).*

It is clear from the data outlined in Table 3, that incorporating a side chain at the 2-position of the benzothiazine scaffold, in general, leads to significant improvements in potency for RORγt and selectivity vs. LXR, particularly LXRβ. Unfortunately, all compounds were potent agonists of PXR. Resolution of enantiomers of compound **25** (**25a** and **25b**) confirmed that the more potent isomer at RORγt was also a potent full agonist of PXR (**25a**). That the lack of selectivity for PXR was not unique to the benzothiazine chemotype was confirmed by the fact that the tetrahydroquinoline chemotype displayed a similar profile (Figure 1).

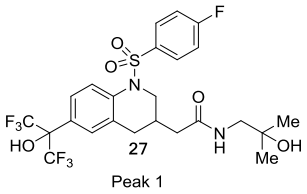

RORγt EC_{50} nM: 15
PXR EC_{50} nM (% max.): 300 (93)

RORγt EC_{50} nM: 1530
PXR EC_{50} nM (% max.): 270 (84)

Figure 1. RORγt and PXR activity of **27** and **28** in reporter assays. Absolute stereochemistry of peaks 1 and 2 not determined..

In order to understand the structural basis for the lack of selectivity of this series of compounds for PXR and provide direction to achieve selectivity, we obtained the X-ray co-crystal structures of 2-substituted benzothiazine **25a** with the LBD's of both RORγt and PXR (Figure 2).

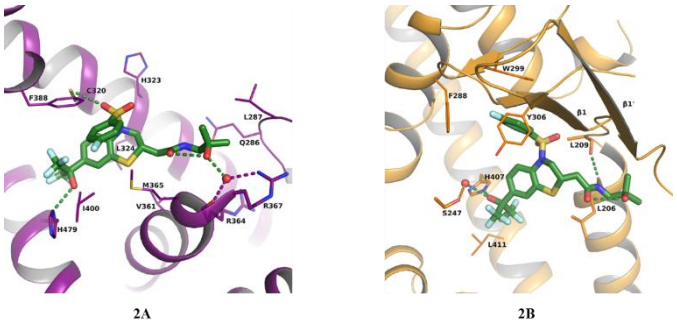

Figure 2. X-ray co-crystal structures of compound **25a** with the LBD of RORγt (2A, PDB ID: 6BN6) and PXR (2B, PDB ID: 6BNS)

The X-ray co-crystal structure of **25a** bound to RORγt was resolved at 2.40 Å, revealing a number of polar interactions and van der Waals contacts between the ligand and the RORγt binding pocket and the absence of electron density for helix 12. The destabilization of helix 12 provides further evidence for the inverse agonist nature of the interaction of compound **25a** with the LBD of RORγt. The hexafluoroisopropyl alcohol forms a hydrogen bond with the side chain of His479,[15] while one of the sulfone oxygens forms a hydrogen bond with the side chain of Cys320. In addition, the hydroxyl group of hydroxypropyl acetamide moiety forms water-mediated hydrogen bonds to the side chain of Arg367 and the backbone carbonyl of Arg364, as well as an intramolecular hydrogen bond to the acetamide carbonyl. The 4-fluorophenyl sulfonamide group occupies a hydrophobic pocket formed by the side chains of Met365, Val376, Phe378, Phe388, Ile400 and Phe401 and forms partial parallel pi stacking interactions with Phe388 (~3.6 Å). Phe388 engages neighboring Phe378 in an edge-to-face pi stacking interaction. The hexafluoroisopropyl group occupies a pocket rich in hydrophobic residues that includes Trp317, Met358, Leu396, Ile397, Ile400 and Leu483. The tetrahedral sulfone group projects the 4-fluorophenyl moiety in a parallel plane to the rest of the ligand, allowing for favorable hydrophobic interactions as discussed above. This orientation cannot be achieved by the amide analog **8**, which is consistent with its lower RORγt potency.

The X-ray co-crystal structure of **25a** bound to PXR was resolved at 2.56 Å. Similar to the structure of **25a** with the LBD of RORγt, both polar interactions and a number of van der Waals contacts are observed between the ligand and the binding pocket of PXR. However, unlike the RORγt structure, there is clear presence of electron density for helix 12 in the PXR structure for compound **25a**. The stabilization of helix 12 provides further evidence for the agonist nature of the interaction of compound **25a** with the LBD of PXR. The hexafluoroisopropyl alcohol moiety forms a hydrogen bond with the side chain of His407 (2.47 Å) and a water-mediated hydrogen bond with the side chain of Ser247. The acetamide NH forms hydrogen bonding interactions with the backbone carbonyls of Leu206 and Leu209. The 4-fluorophenyl sulfone moiety of **25a** occupies a hydrophobic pocket formed by the side chains of Phe288, Trp299, Tyr306, Leu209 and Val211 and is sandwiched between Trp299 in parallel pi stacking interaction with Phe288 and Tyr306. As in the RORγt structure, the hexafluoroisopropyl group is lodged in a pocket rich in hydrophobic residues that includes Phe420, Met425, Leu240 and Leu411. However, unlike the binding orientation of compound **25a** in RORγt where the hydroxypropyl acetamide -OH is involved in a water-mediated hydrogen bond with the side chain of Arg367 and backbone carbonyl of Arg364, the hydroxypropyl acetamide moiety is projected into an open pocket in PXR and is involved in only weak hydrophobic interactions (~3.8 Å range) with residues in loops near Pro227 and Ile236.

The improved potency of compound **25a** for RORγt can be rationalized by the water-mediated hydrogen bond between the hydroxyl group of hydroxypropyl acetamide moiety with the side chain of Arg367, backbone carbonyl of Arg364. A similar kind of the H-bond interaction (with or without water mediation) may explain the improved potency for RORγt, seen for other compounds in Table 3, with polar acetamide side chains compared to compound **1**. However, it was clear from the X-ray co-crystal structures, that compound **25a** was engaging the same polar and hydrophobic interactions with the LBD's of RORγt and PXR: the hydroxyl group of the hexafluoroisopropyl alcohol forms hydrogen bonds with His479 or His407; the 4-fluorophenyl group is lodged in a very hydrophobic pocket; and the hexafluoroisopropyl moiety is lodged in a pocket rich in hydrophobic residues in both RORγt and PXR. This issue was further exaggerated by the fact that the acetamide side chain at the 2-position of the ligand was projecting into an open pocket in PXR, suggesting that modifications in this region of the ligand would be tolerated in PXR, which is consistent with the SAR described above (Table 3).

We also noted that the 4-fluorophenylsulfonyl moiety of compound **25a** assumes a pseudoaxial orientation in the RORγt structure and engages in a pi stacking interaction with the phenyl group anchoring the hexafluoroisopropyl alcohol moiety (*vide supra*). In the PXR structure the 4-fluorophenylsulfonyl moiety adopts a pseudoequatorial orientation, which is similar to what is observed in the single crystal X-ray of compound **25a** (CCDC # 1586092).

Closer examination of the X-ray co-crystal structure of **25a** with the LBD of PXR suggested that moving the side chain from position 2 of the benzothiazine scaffold to position 3 would create a steric clash with the β1 sheet in PXR, potentially improving selectivity while maintaining potency for RORγt. To test this hypothesis, we synthesized compounds in both the benzothiazine and tetrahydroquinoline series. Table 4 outlines the *in vitro* data for this set of compounds.

Table 4. SAR of 3-substituted benzothiazines and 2-substituted tetrahydroquinolines

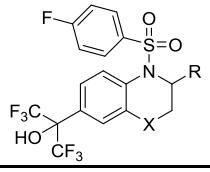

	R	X	RORγt EC_{50} nM[a,b]	PXR EC_{50} nM (% max.)[c]	LXRα EC_{50} nM (% max.)[d]	LXRβ EC_{50} nM (% max.)[d]	HLM/MLM Stability (%)[e]
25		S	31 ± 12	175 (90)	2770 ± 600 (39)	>7500	64, 55
29	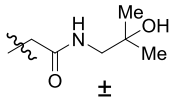	S	97[c]	1510 (83)	792 (100)[c]	>7500[c]	11, 2
30*	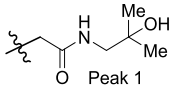	S	32[c]	1100 (90)	>7500	>7500	5, 2
31*	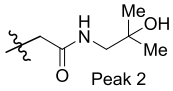	S	7380[c]	1350 (70)	315 (93)[c]	3710[c]	2, 1
32	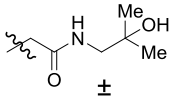	CH_2	47[c]	2000 (80)	1030 (83)[c]	>7500[c]	38, 15
33[†]	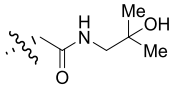	CH_2	15 ± 2	1830 (91)	>7500	>7500	59, 25
34	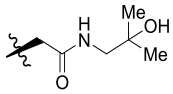	CH_2	7500 ± 1250	2860 (76)	320 (78)[c]	>7500[c]	30, 0.7
35	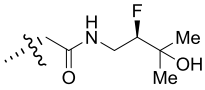	CH_2	39 ± 18	2000 (100)	>7500	>7500	56, 62

[a]Values are means of two or more experiments performed in triplicate. [b]RORγt reporter assay was performed using a Jurkat cell line. [c]Value from a single experiment performed in duplicate. [d]LXR assays (agonist mode) were performed using a CV-1 cell line. [e]Metabolic stability in human and mouse liver microsomes (HLM and MLM). Values are percentage remaining after 10 min. of incubation. [*]Absolute stereochemistry not established. [†]Absolute stereochemistry established by single crystal X-ray (CCDC # 1586093)

It is clear from the data listed in Table 4 that moving the side chain to the 3-position of the benzothiazine or the 2-position of the tetrahydroquinoline scaffold decreases the potency of these compounds for PXR by an order of magnitude (although the Y_{max} remains high), consistent with our hypothesis. Other important SAR points of note are as follows: (a) on resolution of racemic mixtures (**29** and **32**), there is an approximately three fold improvement in potency for RORγt (compare **29** with **30** and **32** with **33**), (b) LXRα activity is eliminated in the more active RORγt enantiomer (compounds **30** and **33**) – all of the LXRα activity resides in the less potent RORγt enantiomer (compounds **31** and **34**). In order to understand the stereochemical preference for LXRα activity with compounds **31** and **34**, we docked compound **34** in hLXRα (PDB ID: 5HJS,[16] Figure 3).

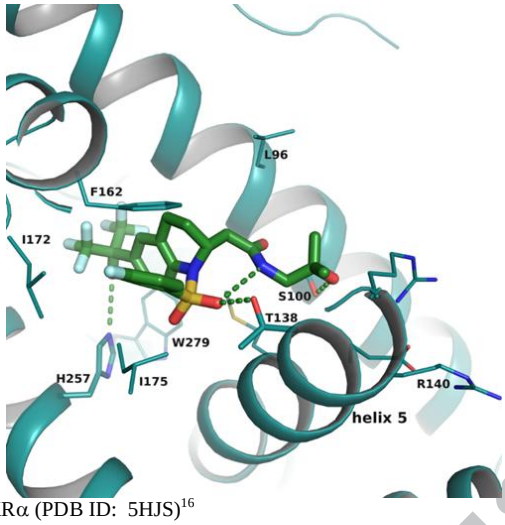

Figure 3. Model of compound **34** docked in hLXRα (PDB ID: 5HJS)[16]

The binding model suggests the hexafluoroisopropyl alcohol forms a hydrogen bond with the side chain of His257 and the 4-fluorophenyl sulfonamide group occupies the hydrophobic pocket formed by the side chains of Ile149, Phe162, Leu167, Phe171, Phe175 and Phe176. One of the sulfonamide oxygens forms a hydrogen bond with the side chain of Thr138 and an intra-molecular hydrogen bond with the acetamide NH. The acetamide moiety extends towards the polar region of the LXRα LBD, allowing the alcohol to form a hydrogen bond with the side chain of Ser100. In contrast to compound **34**, we were unable to dock compounds **30** and **33** in this model. We hypothesize that the "*S*" orientation of the side chain in compounds **30** and **33** cannot be accommodated without an accompanying steric clash with helix 5 in the LBD of hLXRα.

Bioisosteric replacements of the amide (urea, reverse amides, sulfonamides and heterocycles) did not lead significant improvements in RORγt potency and/or selectivity vs. PXR (data not shown). It is of interest to note that moving the side chain from the 2-postion of the benzothiazine scaffold to the 3-position significantly decreases the metabolic stability in the *in vitro* human and mouse liver microsomal assay (Table 4, compare **25** with **29**). Although compound **33** showed a favorable profile in terms of potency for RORγt and selectivity against LXRα/β and PXR, the *in vitro* metabolic stability in the liver microsomal assay was less than desirable for advancement into *in vivo* pharmacodynamic (PD) models. Further SAR studies led to the identification of compound **35**, which had good *in vitro* liver microsomal stability and was advanced to a PD model.

To assess the ability of compound **35** to inhibit RORγt-dependent responses *in vivo*, a short pharmacodynamic model was developed that relied on IL-2 and IL-23 stimulation. Naive mice were challenged three times with IL-2 and IL-23 (at 0, 7, and 23 hours) after IL-2 alone priming (-24 hour). Serum IL-17 was analyzed 7 hour after last IL-2/IL-23 administration. Oral dosing of compound **35** under these conditions significantly blocked the IL-17 response in a dose-dependent manner and achieved 74% inhibition at 25 mg/kg and 98% inhibition at 100 mg/kg doses, respectively (Figure 4). These data demonstrate that systemic administration of RORγt inverse agonist **35** limits IL-17 response *in vivo*.

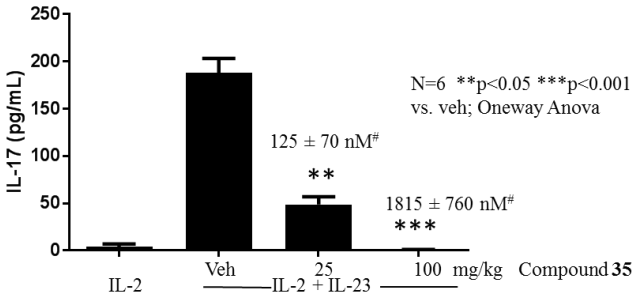

Figure 4. *In vivo* activity of compound **35** in the IL-2/IL-23 induced IL-17 PK-PD model. # Terminal exposures from study.

Encouraged by the favorable results from the PD study, the next step was to test compound **35** in chronic mouse models of autoimmune disorders. Before embarking on testing the compound in preclinical *in vivo* models, we decided to do a five day PK study. Although the potency of compound **35** was significantly right shifted in the PXR assay (*vide supra*), the high Y_{max} suggested that the compound can potentially act as a full agonist of PXR at concentrations above 2 μM. Since activity in the PXR assay suggests the potential to induce human Cyp3A4, we wanted to know if Cyp3a11 (mouse equivalent of Cyp3A4) is induced in an *in*

vitro mouse hepatocyte assay. In the event, when compound **35** was tested in the mouse hepatocyte assay, Cyp3a11 was upregulated 21-, 47- and 40-fold at concentrations of 1, 3 and 10 μM, respectively, when compared to DMSO control. Although we did not conduct reaction phenotyping studies to understand the Cyp enzyme responsible for the metabolism of compound **35**, the induction of Cyp3a11 in *in vitro* studies suggested the potential for auto-induction leading to decrease in exposures upon repeat dosing. A mouse PK study was conducted at oral doses of 30 mg/kg and 100 mg/kg of compound **35** twice daily for five days. Exposures at day 1 and day 5 were recorded and the data are summarized in Tables 5A and 5B.

Table 5A[#]

Compound **35** concentration at 30 mg/kg, PO, BID* (nM)					
	Day 1		Day 5		Fold decrease
Time (h)	Mean	SD	Mean	SD	
1	3488	782	555	175	6.3
7.5	134	35	21	19	6.5
23.5	5	-	5	-	1.0

Table 5B[#]

Compound **35** concentration at 100 mg/kg, PO, BID* (nM)					
	Day 1		Day 5		
Time (h)	Mean	SD	Mean	SD	
1	13895	1916	2834	1239	4.9
7.5	2460	1250	61	37	40
23.5	19	9	-	-	-

[#] *PK protocol: mouse PK studies were conducted in male Balb/c mice. *vehicle for PK study: 55% PEG300/25%Proplylene glycol/10%TPGS/10%water.*

Comparing day 1 and day 5 exposures, it is clear from the data in Tables 5A/5B that there is ~5-6 fold drop in exposure at 1 h and ~7-40 fold drop in exposure at 7.5 h at both the 30 mg/kg and 100 mg/kg doses. At the end of the study, liver tissue samples were collected and evaluated for Cyp3a11 mRNA levels. Consistent with the *in vitro* data, a dose dependent increase in Cyp3a11 mRNA levels were observed (~3.5 and 5.5 fold increase over dosing vehicle group at 30 mg/kg and 100 mg/kg respectively). Although one cannot rule out the possibility of alteration of other clearance mechanisms causing the reduced exposure on chronic dosing, the strong *in vitro-in vivo* correlation suggests that increased Cyp3a11 expression may be a significant factor contributing to the reduction in exposure due to auto-induction by compound **35**. The loss in exposure in the five-day PK study limited our ability to test compound **35** in chronic preclinical models of autoimmune disorders.

Synthetic approaches to compounds in Tables 1-4 and Figure 1 are outlined in Schemes 1-7. The hexafluoroisopropyl alcohol moiety present in all the final compounds was introduced by alkylating an aniline substrate with hexafluoroacetone hydrate at high temperature. The key steps in the preparation of compounds **27** and **28** were a Heck-type palladium mediated reaction of 3-bromoquinoline (**44**) with a silyl enol ether, followed by selective hydrogenation of the quinoline ring using PtO_2. The key step in the preparation of compound **35** is the Horner–Wadsworth–Emmons reaction of the aminal **52** with triethyl phosphonoacetate to form an acrylate, which undergoes an intramolecular Michael reaction via a favorable six exo-trig process to provide the tetrahydroquinoline derivative **53** following Boc deprotection.[17]

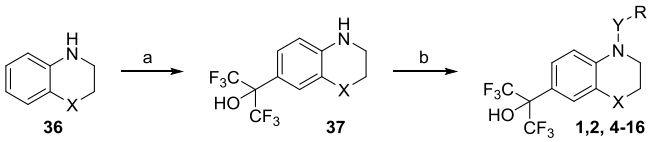

Scheme 1 Conditions: (a) (1) hexafluoropropan-2-one, microwave, 160 °C, 10 min.; (2) silica gel chromatography to separate regioisomers, 43%; (b) RSO_2Cl, pyridine, DCM or RCOCl, DMAP, DCM or RCH_2Br, NaH, DMSO.

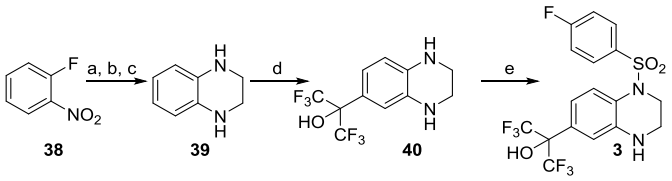

Scheme 2 Conditions: (a) methyl 2-aminoacetate hydrochloride, Et_3N, DMF, 80 °C, 64%; (b) H_2, Pd/C, MeOH, 40 psi, RT, 97%; (c) LAH, RT, 12 h, 64%; (d) hexafluoropropan-2-one, PTSA, microwave, 45 min., 80 °C, prep. HPLC to separate regioisomers, 41%; (e) 4-fluorobenzenesulfonyl chloride, pyridine, DCM, Prep. HPLC to separate regioisomers, 4%.

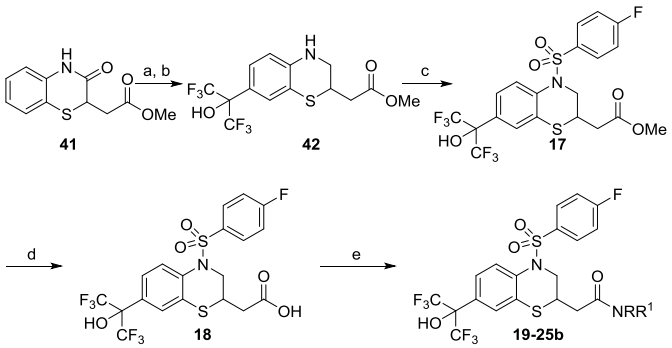

Scheme 3 Conditions: (a) BH_3, THF, 78%; (b) hexafluoropropan-2-one, PTSA, 100 °C, 12 h, 46%; (c) 4-fluorobenzenesulfonyl chloride, pyridine, DCM, RT, 12 h, 32%; (d) LiOH, THF, H_2O, RT, 1 h, 90%; (e) RR_1NH, BOP, DMF, DIPEA.

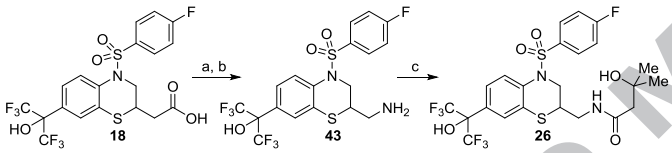

Scheme 4 Conditions: (a) DPPA, Et_3N, 2-(trimethylsilyl)ethan-1-ol, 100 °C, 30 min., 65%; (b) TBAF, THF, RT, 2 h, 90%; (c) BOP, DMF, DIPEA, RT, 1 h, 50%.

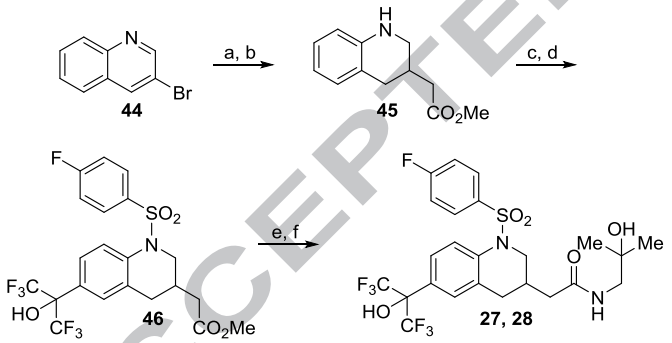

Scheme 5 Conditions: (a) tert-butyl((1-methoxyvinyl)oxy)dimethylsilane, $Pd(Tol_3P)_2Cl_2$, KOAc, toluene, 110 °C, 30 h, 72%; (b) PtO_2, H_2, MeOH, 70%; (c) hexafluoropropan-2-one, PTSA, microwave, 40 min., 70 °C, 61%; (d) 4-fluorobenzenesulfonyl chloride, pyridine, DCM, 24 h, 58%; (e) LiOH, THF, H_2O, RT, 3 h, 86%; (f) HATU, DIPEA, DMF, RT, 3 h, Chiralcel OD-H column.

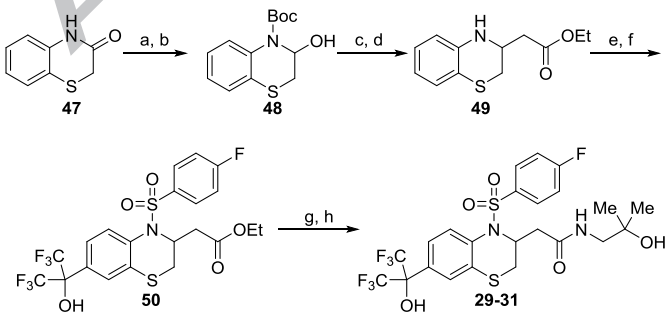

Scheme 6 Conditions: (a) $[(CH_3)_3COCO]_2O$, DMAP, CH_3CN, RT, 15 h, 100%; (b) $LiEt_3BH$, THF, -78 °C, 30 min.; (c) triethyl phosphonoacetate, NaH, THF, 79% (over two steps); (d) TFA, DCM; (e) hexafluoropropan-2-one, PTSA, 120 °C, 12 h, 47% (over two steps); (f) 4-fluorobenzenesulfonyl chloride, pyridine, DCM, RT, 15 h, 55%; (g) LiOH, THF, H_2O, RT, 2 h, (40%); (h) (1) BOP, DIPEA, DMF, RT, 1 h, 31%; (2) Whelk-O1 (R.R) chiral column.

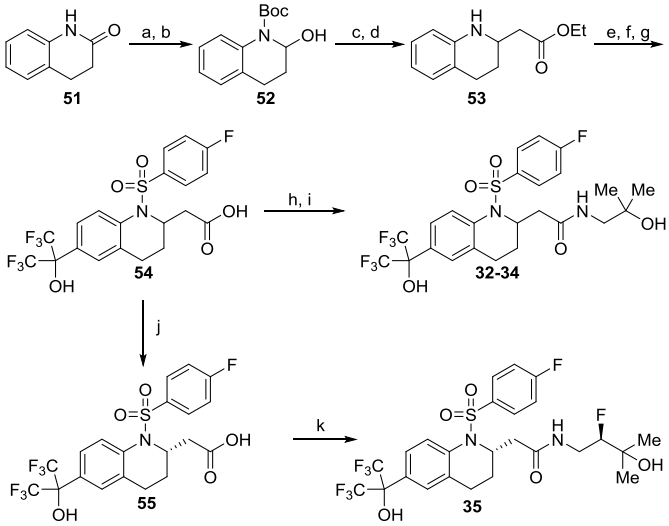

Scheme 7 Conditions: (a) $[(CH_3)_3COCO]_2O$, DMAP. CH_3CN, RT, 20 h, 95%; (b) $LiEt_3BH$, THF, -78 ^oC, 30 min.; (c) triethyl phosphonoacetate, NaH, THF, 67% (over two steps); (d) TFA, DCM, 1 h, 99%; (e) hexafluoropropan-2-one, PTSA, 120 ^oC, 3 h; (f) 4-fluorobenzenesulfonyl chloride, pyridine, DCM, RT, 15 h, 41% over two steps; (g) LiOH, THF, H_2O, RT, 15 h; (h) BOP, DIPEA, DMF, RT, 1 h, 67%; (i) Whelk-O1 (R.R) chiral column; (j) Whelk-O1 (R.R) chiral column, absolute configuration of **55** determined by single crystal X-ray (CCDC # 1586094); (k) (S)-4-amino-3-fluoro-2-methylbutan-2-ol,[18] BOP, DIPEA, DMF, RT, 1 h, 58%.

In conclusion, a HTS screen of the BMS compound collection led to the identification of benzothiazine analog **1**, which exhibited modest activity for RORγt but poor selectivity for PXR and LXRα/β in cell-based functional assays. We were able to significantly improve RORγt potency while reducing LXRβ activity by conducting SAR studies at the 2-position of the benzothiazine scaffold. However, these compounds were still significantly potent at PXR and showed moderate activity at LXRα. We solved the X-ray co-crystal structures of a 2-substituted benzothiazine (**25a)** with the LBDs of RORγt and PXR. Based on these structures, we developed SAR in a 3-substituted benzothiazine and 2-substituted tetrahydroquinoline series. Representative compound **35** maintained potency at RORγt and exhibited markedly improved selectivity for PXR and LXRα. Furthermore, compound **35** demonstrated dose-dependent inhibition of IL-17 when tested *in vivo* in an IL-2/IL-23 induced IL-17 PD model. However, we were unable to test compound **35** in chronic mouse models of autoimmunity due to significant drop in exposures on repeat dosing in a mouse PK study, likely due to compound-induced upregulation of Cyp3a11 (mouse 3A4 counterpart). Further work to minimize the PXR activity and increase RORγt potency of this series of RORγt inverse agonists is in progress in our laboratories and will be reported in due course.

References and Notes

1. Cook DN, Kang HS, Jetten AM. Retinoic acid-related orphan receptors (RORs): Regulatory functions in immunity, development, circadian rhythm, and metabolism. *Nucl. Receptor Res*. 2016; 2: Article ID 101185.
2. Ivanov II, McKenzie BS, Zhou L, Tadokoro CE, Lepelley A, Lafaille JJ, Cua DJ, Littman DR. The orphan nuclear receptor RORγt directs the differentiation program of proinflammatory IL-17+ T helper cells. *Cell* 2006; 126: 1121-1133.
3. (a) Chabaud M, Durand JM, Buchs N, Fossiez F, Page G, Frappart L, Miossec P. Human Interleukin-17: A T cell-derived proinflammatory cytokine produced by the rheumatoid synovium. *Arthritis Rheum*. 1999; 42: 963−970. (b) Lock C, Hermans G, Pedotti R, Brendolan A, Schadt E, Garren H, Langer-Gould A, Strober S, Cannella B, Allard J, Klonowski P, Austin A, Lad N, Kaminski N, Galli SJ, Oksenberg JR, Raine CS, Heller R, Steinman L. Gene-microarray analysis of multiple sclerosis lesions yields new targets validated in autoimmune encephalomyelitis. *Nat. Med*. 2002; 8: 500−508. (c) Fujino S, Andoh A, Bamba S, Ogawa A, Hata K, Araki Y, Bamba T, Fujiyama Y. Increased expression of interleukin 17 in inflammatory bowel disease. *Gut*. 2003; 52: 65−70. (d) Seiderer J, Elben I, Diegelmann J, Glas J, Stallhofer J, Tillack C, Pfennig S, Jürgens M, Schmechel S, Konrad A, Göke B, Ochsenkühn T, Müller-Myhsok B, Lohse P, Brand S. Role of the novel Th17 cytokine IL-17F in inflammatory bowel disease (IBD): Upregulated colonic IL-17F expression in active Crohn's disease and analysis of the IL17F p.His161Arg polymorphism in IBD. *Inflamm. Bowel Dis*. 2008; 14: 437−445.
4. Dhar TGM, Zhao Q, Markby DW. Targeting the nuclear hormone receptor RORγt for the treatment of autoimmune and inflammatory disorders. *Annu. Rep. Med. Chem*. 2013; 48: 169−182.
5. (a) Skepner J, Ramesh R, Trocha M, Schmidt D, Baloglu E, Lobera M, Carlson T, Hill J, Orband-Miller LA, Barnes A, Boudjelal M, Sundrud M, Ghosh S, Yang J. Pharmacologic inhibition of RORγt regulates Th17 signature gene expression and suppresses cutaneous inflammation in vivo. *J. Immunol*. 2014; 192: 2564-2575. (b) Banerjee D, Zhao L, Wu L, Palanichamy A, Ergun A, Peng L, Quigley C, Hamann S, Dunstan R, Cullen P, Allaire N, Guertin K, Wang T, Chao J, Loh C, Fontenot JD. Small molecule mediated inhibition of RORγ-dependent gene expression and autoimmune disease pathology in vivo *Immunology*. 2016; 147: 399-413. (c) Xue X, Soroosh P, De Leon-Tabaldo A, Luna-Roman R, Sablad M, Rozenkrants N, Yu J, Castro G, Banie H, Fung-Leung WP, Santamaria-Babi L, Schlueter T, Albers M, Leonard K, Budelsky AL, Fourie AM. Pharmacologic modulation of RORγt translates to efficacy in preclinical and translational models of psoriasis and inflammatory arthritis. *Sci. Rep*. 2016; *6*: Article number: 37977. (d) Smith SH, Peredo CE, Takeda Y, Bui T, Neil J, Rickard D, Millerman E, Therrien JP, Nicodeme E, Brusq JM, Birault V, Viviani F, Hofland H, Jetten AM, Cote-Sierra J. Development of a topical treatment for psoriasis targeting RORγ: From Bench to Skin. *PLoS One*. 2016; *11*:

e0147979. (e) Takaishi M, Ishizaki M, Suzuki K, Isobe T, Shimozato T, Sano S. *J. Dermatol. Sci*. 2017; *85*: 12-19.

6. (a) de Wit J, Al-Mossawi MH, Hühn MH, Arancibia-Cárcamo CV, Doig K, Kendrick B, Gundle R, Taylor P, Mcclanahan T, Murphy E, Zhang H, Barr K, Miller JR, Hu X, Aicher TD, Morgan RW, Glick GD, Zaller D, Correll C, Powrie F, Bowness P. RORγt inhibitors suppress T(H)17 responses in inflammatory arthritis and inflammatory bowel disease. *J. Allergy Clin. Immunol.* 2016; 137: 960-963. (b) Withers DR, Hepworth MR, Wang X, Mackley EC, Halford EE, Dutton EE, Marriott CL, Brucklacher-Waldert V, Veldhoen M, Kelsen J.; Baldassano RN, Sonnenberg GF. Transient inhibition of RORγt therapeutically limits intestinal inflammation by reducing TH17 cells and preserving group 3 innate lymphoid cells. *Nat. Med*. 2016; 3: 319-323.

7. Chang MR, Lyda B, Kamenecka TM, Griffin, PR. Pharmacologic repression of retinoic acid receptor-related orphan nuclear receptor γ is therapeutic in the collagen-induced arthritis experimental model. *Arthritis Rheumatol*. 2014; 3: 579-588.

8. (a) Wang Y, Cai W, Zhang G, Yang T, Liu Q, Cheng Y, Zhou L, Ma Y, Cheng Z, Lu S, Zhao YG, Zhang W, Xiang Z, Wang S, Yang L, Wu Q, Orband-Miller LA, Xu Y, Zhang J, Gao R, Huxdorf M, Xiang, JN, Zhong Z, Elliott JD, Leung S, Lin X. Discovery of novel N-(5-(arylcarbonyl)thiazol-2-yl)amides and N-(5-(arylcarbonyl)thiophen-2-yl)amides as potent RORγt inhibitors. *Bioorg. Med. Chem.* 2014; 22: 692-702. (b) Yang Y, Winger RC, Lee PW, Nuro-Gyina PK, Minc A, Larson M, Liu Y, Pei W, Rieser E, Racke MK, Lovett-Racke AE. Impact of suppressing retinoic acid-related orphan receptor gamma t (RORγt) in ameliorating central nervous system autoimmunity. *Clin. Exp. Immunol.* 2015; 179: 108-118. (c) Wang Y, Cai W, Cheng Y, Yang T, Liu Q, Zhang G, Meng Q, Han F, Huang Y, Zhou L, Xiang Z, Zhao YG, Xu Y, Cheng Z, Lu S, Wu Q, Xiang JN, Elliott JD, Leung S, Ren F, Lin X. Discovery of biaryl amides as potent, orally bioavailable, and CNS penetrant RORγt inhibitors. *ACS Med. Chem. Lett.* 2015; 6: 787-792.

9. (a) Fauber BP, Magnuson S. Modulators of the nuclear receptor retinoic acid receptor-related orphan receptor-γ (RORγ or RORc). *J. Med. Chem.* 2014; 57: 5871−5892. (b) Kojetin DJ, Burris TP. REV-ERB and ROR nuclear receptors as drug targets. *Nat. Rev. Drug Discovery*. 2014; *13*: 197-216. (c) Zhang Y, Luo XY, Wu DH, Xu Y. ROR nuclear receptors: structures, related diseases, and drug discovery. *Acta Pharmacologica Sinica*. 2015; 36: 71–87. (d) Cyr P, Bronner SM, Crawford JJ. Recent progress on nuclear receptor RORγ modulators. *Bioorg. Med. Chem. Lett*. 2016; 26: 4387-4393. (d) Bronner SM, Zbieg JR, Crawford JJ. RORγ antagonists and inverse agonists: a patent review. *Expert Opin. Ther. Pat.* 2017; *27*: 101-112.

10. (a) Kumar N, Lyda B, Chang Mi Ra Lauer, JL, Solt LA, Burris TP, Kamenecka TM, Griffin PR. Identification of SR2211: A potent synthetic RORγ-selective modulator. *ACS Chem. Biol*. 2012; 7: 672−677. (b) Huh JR, Englund EE, Wang H, Huang R, Huang P, Rastinejad F, Inglese J, Austin CP, Johnson RL, Huang W, Littman DR, Identification of potent and selective diphenylpropanamide RORγ inhibitors. *ACS Med. Chem. Lett*., 2013; 4: 79-84. (c) Muegge I, Collin D, Cook B, Hill-Drzewi M, Horan J, Kugler S, labadia M, Li X, Smith L, Zhang Y. Discovery of 1,3-dihydro-2,1,3-benzothiadiazole 2,2-dioxide analogs as new RORC modulators. *Bioorg. Med. Chem. Lett*. 2015; 25: 1892-1895. (d) Wang Y, Yang T, Liu Q, Ma Y, Yang L, Zhou L, Xiang Z, Cheng Z, Lu S, Orband-Miller LA, Zhang W, Wu Q, Zhang K, Li Y, Xiang JN, Elliott, JD, Leung S, Ren F, Lin X. Discovery of N-(4-aryl-5-aryloxy-thiazol-2-yl)-amides as potent RORγt inverse agonists. Bioorg. Med. Chem. Lett. 2015; 25: 5293-5302. (e) Scheepstra M, Leysen S, van Almen GC, Miller JR, Piesvaux J, Kutilek V, van Eenennaam H, Zhang H, Barr K, Nagpal S, Soisson SM, Kornienko M, Wiley K, Elsen N, Sharma S, Correll CC, Trotter BW, van der Stelt M, Oubrie A, Ottmann C, Parthatsarathy G, Brunsveld L. Identification of an allosteric binding site for RORγt inhibition. *Nat. Commun*., 2015; 7: 8833. (f) Enyedy I, Powell N, Caravella J, Vloten KV, Chao J, Banerjee D, Marcotte D, Silvian L, McKenzie A, Hong VS, Fontenot J. Discovery of biaryl carboxylamides as potent RORγ inverse agonists. *Bioorg. Med. Chem. Lett.* 2016; *26*: 2459–2463. (g) Olsson RI, Xue Y, Von Berg S, Aagaard A, McPheat J, Hansson EL, Bernstrom J, Hansson P, Jirholt J, Grindebacke H, Leffler A, Chen R, Xiong Y, Ge H, Hansson T, Narjes F. Benzoxazepines achieve potent suppression of IL-17 release in human T-Helper 17 (TH17) cells through an induced-fit binding mode to the nuclear receptor RORγ. *ChemMedChem.* 2016; *11*: 207-216. (h) Rene O, Fauber BP, Barnard A, Chapman K, Deng Y, Eidenschenk C, Everett C, Gobbi A, Johnson AR, La H, Norman M, Salmon G, Summerhill S, Wong H. Discovery of oxa-sultams as RORc inverse agonists showing reduced lipophilicity, improved selectivity and favorable ADME properties. *Bioorg. Med. Chem. Lett.* 2016; 26: 4455-4461. (i) Hirata K, Kotoku M, Seki N, Maeba T, Maeda K, Hirashima S, Sakai T Obika S, Hori A, Hase Y, Yamaguchi T, Katsuda Y, Hata T, Miyagawa N, Arita K, Nomura Y, Asahina K, Aratsu Y, Kamada M, Adachi T, Noguchi M, Doi S, Crowe P, Bradley E, Steensma R, Tao H, Fenn M, Babine R., Li X, Thacher S, Hashimoto H, Shiozaki M. SAR exploration guided by LE and Fsp3: discovery of a selective and orally efficacious RORγ inhibitor. *ACS Med. Chem. Lett*. 2016; 7: 23−27. (j) Hintermann S, Guntermann C, Mattes H, Carache DA, Wagner J, Vulpetti A, Billich A, Dawson J, Kaupmann K, Kallen J, Stringer R, Orain D. Synthesis and biological evaluation of new triazolo- and imidazolopyridine RORγt inverse agonists. *ChemMedChem* 2016; 11: 2640-2648. (k) Ouvry G, Bouix-Peter C, Ciesielski F, Chantalat L, Christin O, Comino C, Duvert D, Feet C, Harris CS, Lamy L, Luzy AP, Musicki B, Orfila D, Pascau J, Parnet V, Perrin A, Pierre R, Polge G, Raffin C, Rival Y, Taquet N, Thoreau E, Hennequin LF. Discovery of phenoxyindazoles and phenylthioindazoles as RORγ inverse agonists. *Bioorg. Med. Chem. Lett.* 2016; 26: 5802-5808. (l) Kummer DA, Cummings MD, Abad M, Barbay J, Castro G, Wolin R, Kreutter KD, Maharoof U, Milligan C, Nishimura R, Pierce J, Schalkhihi C, Spurlino J, Urbanski M, Venkatesan H, Wang A, Woods C, Xue, X, Edwards JP, Fourie AM, Leonard K. Identification and structure activity relationships of quinoline tertiary alcohol modulators of RORγt. *Bioorg. Med. Chem. Lett*. 2017; 27: 2047-2057.

11. (a) Zhuang L. Discovery of VTP-43742, A RORγt inverse agonist for the treatment of psoriasis. 13th Winter conference on medicinal and bioorganic chemistry, Steamboat Springs, CO. January 22-26, 2017. (b) http://ir.vitaepharma.com/phoenix.zhtml?c=219654&p=irol-newsArticle&ID=2149044 (accessed June 18, 2017).

12. (a) Study of Safety and Efficacy of Topical GSK2981278 Ointment in Plaque Psoriasis. https://clinicaltrials.gov/ct2/show/NCT02548052 (accessed October 1, 2017). (b) Arrien Pharmaceuticals Initiated Phase I Clinical Trials of ARN-6039 as a New Agent for Treatment of Multiple Sclerosis (MS). http://www.businesswire.com/news/home/20160603005095/en/Arrien-Pharmaceuticals-Initiated-Phase-Clinical-Trials-ARN-6039 (accessed October 1, 2017). (c) Safety, Tolerability and Pharmacokinetics of Escalating Single Doses of TAK-828 in Healthy Participants. https://clinicaltrials.gov/ct2/show/NCT02706834 (accessed October 1, 2017). (d) Study to Evaluate Safety, Tolerability, Pharmacodynamics & Pharmacokinetics of JTE-451 in Active Plaque Psoriasis Subjects. https://clinicaltrials.gov/ct2/show/NCT03018509 (accessed October 1, 2017). (e) (e) A Study to Evaluate the Pharmacokinetics, Safety and Tolerability of ABBV-553 in Healthy Volunteers and in Subjects With Psoriasis and Efficacy of ABBV-553 in Subjects With Psoriasis. https://clinicaltrials.gov/ct2/show/NCT02706834 (accessed October 1, 2017).

13. Janowski BA, Willy PJ, Devi TR, Falck JR, Mangelsdorf DJ. An oxysterol signalling pathway mediated by the nuclear receptor LXR alpha. *Nature* 1996; *383*: 728−731.

14. Zhu Z, Puglisi J, Connors D, Stewart J, Herbst J, Marino A, Sinz, M, O'Connell J, Banks M, Dickinson K, Cacace A. Use of cryopreserved transiently transfected cells in high-throughput pregnane X receptor transactivation assay. *J. Biomol. Screen*. 2007; 12: 248-254.

15. Fauber BP, de Leon Boenig G, Burton B, Eidenschenk C, Everett C, Gobbi, A, Hymowitz SG, Johnson A, Limatta M, Lockey P, Norman M, Ouyang W, René O, Wong, H. Structure-based design of substituted hexafluoroisopropanol-arylsulfonamides as modulators of RORc. *Bioorg. Med. Chem. Lett.* 2013; 23: 6604−6609.

16. Stachel SJ, Zerbinatti C, Rudd MT, Cosden M, Suon S, Nanda KK, Wessner K, DiMuzio J, Maxwell J, Wu Z, Uslaner JM, Michener MS, Szczerba P,

Brnardic, E, Rada,V, Kim Y, Meissner R, Wuelfing P, Yuan Y, Ballard J, Holahan M, Klein DJ, Lu J, Frader, X, Parthasarathy G, Uebele VN, Chen Z, Li Y, Li J, Cooke AJ, Bennett DJ, Bilodeau MT, Renger J. Identification and in vivo evaluation of liver X receptor β-selective agonists for the potential treatment of alzheimer's disease. *J. Med. Chem*. 2016; 59: 3489−3498.

17. Perron J, Joseph B, Merour JY. Synthesis of Substituted Azepino[3,4-b]indole-1,5-diones. *Eur. J. Org. Chem*. 2004; 22: 4606-4613.

18. Bhide RS, Duncia JV, Hynes J, Nair SK, Pitts WJ, Kumar SR, Gardner DS, Murugesan N, Paidi,VR, Santella JS, Sistla R, Wu H. Bicyclic Heterocyclic Substituted Pyridyl Compounds Useful as Kinase Modulators. U. S. Patent 9,546,153, January 17, 2017.

Graphical Abstract

To create your abstract, type over the instructions in the template box below.
Fonts or abstract dimensions should not be changed or altered.

Identification of Bicyclic Hexafluoroisopropyl Alcohol Sulfonamides as Retinoic Acid Receptor-Related Orphan Receptor Gamma (RORγ/RORc) Inverse Agonists. Employing Structure-Based Drug Design to Improve Pregnane X Receptor (PXR) Selectivity

Leave this area blank for abstract info.

Hua Gong,[a] David S. Weinstein,[a] Zhonghui Lu,[a] James J.-W. Duan,[a] Sylwia Stachura,[a] Lauren Haque,[a] Ananta Karmakar,[b] Hemalatha Hemagiri,[b] Dhanya Kumar Raut,[b] Arun Kumar Gupta,[b] Javed Khan,[a] Dan Camac,[a] John S. Sack,[a] Andrew Pudzianowski,[a] Dauh-Rurng Wu,[a] Melissa Yarde,[a] Ding-Ren Shen,[a] Virna Borowski,[a] Jenny H. Xie,[a] Huadong Sun,[a] Celia D'Arienzo,[a] Marta Dabros,[a] Michael A. Galella,[a] Faye Wang,[a] Carolyn A. Weigelt,[a] Qihong Zhao,[a] William Foster,[a] John E. Somerville,[a] Luisa M. Salter-Cid,[a] Joel C. Barrish,[a] Percy H. Carter[a] and T. G. Murali Dhar*[a]